Macromolecules

pubs.acs.org/Macromolecules

Article

Time-Domain NMR Elucidates Fibril Formation in Methylcellulose Hydrogels

Denise Besghini, Michele Mauri,* Payam Hashemi, Matthias Knarr, Roland Adden, Petra Mischnick, and Roberto Simonutti

Cite This: *Macromolecules* 2023, 56, 4694−4704

Read Online

ACCESS | Metrics & More | Article Recommendations | Supporting Information

Downloaded via 107.178.192.66 on April 2, 2024 at 07:21:47 (UTC).
See https://pubs.acs.org/sharingguidelines for options on how to legitimately share published articles.

ABSTRACT: The reversible gelation of aqueous methylcellulose (MC) solutions at high temperature is followed stepwise with low-field time-domain nuclear magnetic resonance (LF-TD-NMR). The gel transition does not influence the self-diffusion coefficient of water but is associated with a decrease of proton transverse relaxation times ^1H T_2 by more than 60%. The effect of molecular weight and concentration of polysaccharide chains on transition temperature and gel strength is probed on several MCs with the same degree of substitution. The measured trends connect the NMR relaxation with macroscopic observables and agree with literature results from more demanding techniques like small-angle X-ray and neutron scattering (SAXS and SANS). These findings support the idea of a network structure of disorderly arranged fibrils, with an inhomogeneous mesh size at least on the order of tens of microns, which is in accord with the opaque appearance of these hydrogels. Magic sandwich echo (MSE) NMR measurements performed at 80 °C by substituting water with D_2O also reveal the appearance with thermogelation of a rigid fraction involving about 25% of MC. This is consistent with the formation of fibrils mostly constituted by an amorphous matrix strongly permeated by water and strengthened by well-dispersed MC crystallites.

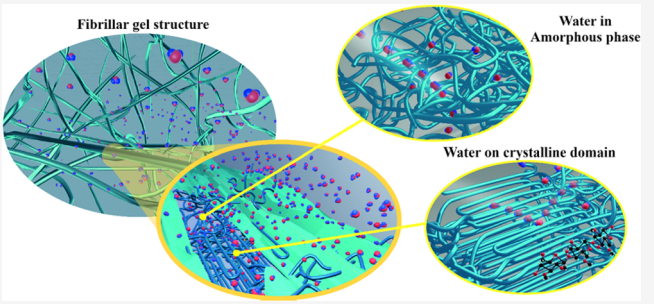

INTRODUCTION

Cellulose derivatives constitute a broad class of materials produced from native cellulose by substituting a fraction of hydroxyl groups along the chain backbone with various chemical moieties.[1,2] Methylcellulose (MC), a partially methyl-substituted cellulose ether (see Figure 1), is widely

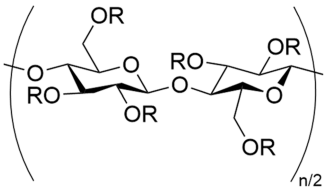

Figure 1. Structure of methylcellulose. The group R can be either a hydrogen atom or a methyl group, depending on the degree of substitution (DS), i.e., the number of substituted OH per glucosyl unit.

employed in formulations as a thickener or binder in the biomedical, cosmetic, textile, architecture, and food industry due to its environmental friendliness, biocompatibility, and biodegradability.[3] The degree of substitution, which can vary from 0 to 3 and is typically about 1.6−2.1, is tailored to tune its properties and especially its peculiar capability to be soluble at room temperature while forming a turbid hydrogel at elevated temperature.[4,5] This physical thermogelation of MC is reversible, and both the gelation process and final gel properties can be controlled by many factors,[6] such as molecular weight,[7,8] concentration,[9,10] substitution pattern,[11−13] the presence and type of salt,[14,15] heating rate,[16] and degree of deuteration of water.[17]

The mechanism of gelation in these systems has been widely debated since the early decades of 1900.[16,18−21] Recent discoveries highlighted that gelation in these systems proceeds through the self-assembly of MC chains into fibrils,[22−24] constituted by 40% of MC and 60% of water, with a diameter of approx. 14−20 nm and a persistence length of 60−200 nm.[23] Following the results of Arvidson et al.,[25] the aggregation is driven by a liquid−liquid phase separation that results in a nucleation and growth mechanism of structures within the polymer-rich phase, where the hydrophobic interaction between the methyl groups[26] is favored. These concurrent mechanisms produce a network formed by a polymer-rich phase, trapping the polymer-lean phase mostly consisting of solvents. Several studies, including molecular dynamics

Received: December 20, 2022
Revised: May 5, 2023
Published: June 5, 2023

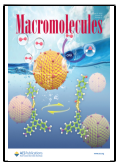

© 2023 The Authors. Published by American Chemical Society

simulations,[11,20,26−28] support the idea that the polysaccharide chains align along the fibril axis, thus forming semicrystalline regions. The formation of fibrils with crystals having a structure like native cellulose has been proposed as the origin of an X-ray scattering diameter that is completely independent of any parameter, such as temperature, concentration, or molecular weight of MC, and with values close to the persistence length of MC chains.[29] The fibrils are then able to entangle and percolate, originating strong interconnected gels with high moduli[7,30] and heterogeneous distribution of mesh size varying from 20 to 100 nm.[31]

Many techniques have been used so far to investigate MC gelation, namely, differential scanning calorimetry (DSC),[32] rheology,[30] dynamic and static light scattering,[20,24] small-angle X-ray and neutron scattering (SAXS and SANS),[7,21,29,33] and cryo-TEM;[24] few studies have employed nuclear magnetic resonance (NMR).[17,21,31] Using high-field instruments, it was possible to focus on MC molecules, analyzing the changes in intensity and increasing the width of peaks attributed to MC with temperature. In fact, during the gelation, MC proton dynamics becomes hindered because of their association.[31] Further insight on dynamics can be obtained by time-domain experiments. So far, no one reported low-field time-domain NMR (LF-TD-NMR) investigation of solvent relaxation on MC "hot-gels".

Here, we present, to the best of our knowledge, the first study of MC thermogelation in water for different concentrations and molecular weights but with the same DS and methyl pattern. First, we confirmed the suitability of the relaxometric parameter T_2 for detecting MC sol−gel transition. Through extensive relaxometric studies, we reproduced the observations already made through other techniques, such as the independence of the gel point from M_w, its dependence on concentration, and the hysteresis of the gel−sol transition. Then, with the measurement of the parameters T_1 and D, we discussed the water dynamics in these systems throughout the gelation process at different time scales. Finally, we applied the advanced magic sandwich echo (MSE) refocusing block to directly probe the internal morphology of the fibrils, measuring a rigid fraction attributed to MC crystals that impart mechanical stability to a highly swollen amorphous phase.

MATERIALS AND METHODS

Materials. Samples of methylcellulose with the same DS 1.92 (Zeisel) have been used. These MC samples were kindly provided by International Flavors & Fragrances (IFF), Pharma Solutions, and are labeled MC1 to MC4 in ascending degree of viscosity. MC1−3 are all derived from MC4 by partial hydrolysis to reduce molecular weight and viscosity. Therefore, all MCs have the same DS and the same substitution pattern. Deionized water for the preparation of samples was obtained from a Millipore water purification system. D_2O was purchased from Sigma-Aldrich with 99.9% deuterium atoms.

Solution Preparation Method. MC powder materials were dried in a vacuum oven at 60 °C overnight and then kept in a desiccator under nitrogen at room temperature. To prepare the aqueous solution of MC with 0.5, 1, 2, 3, 4, and 5% w/w concentration, the calculated quantity of dry MC was put in a vial with a PTFE magnetic stirrer bar and deionized water was added to reach half the total weight of the final solution. The vials were, then, capped and the dispersions were stirred at 80 °C for 30 min and at 70 °C for another 30 min. At this point, dispersions were cloudy but almost uniform. Thereafter, each vial was topped with the remaining required half of ice-cold deionized water and placed in an ice bath while being stirred by a magnet stirrer and occasionally by a strong vortex mixer. In less than 2 min after the addition of the ice-cold, all of the solutions started to become transparent; and in 7−10 min, they all looked homogeneous and exhibited viscosity. Stirring on an ice bath and vortexing were continued for a total of 1 h. Then, the samples were kept in a refrigerator at 4 °C for 48 h for complete hydration. For the highest concentrations, additional waiting time in the refrigerator was needed to allow for all of the air bubbles trapped in the highly viscous solutions to disappear.

The same procedure was followed for preparing 1 mL of 3% MC1 solution in D_2O. This concentration has been chosen to balance the necessity of a high enough signal during NMR measurements and ease of solution preparation. Before the analysis, the solution was sealed and kept in the refrigerator for some days to allow for complete hydration and exchange of D atoms with MC exchangeable H.

Rheology. For assessment of the viscosity shear rate dependence of the samples, these have been hydrated in an aqueous solution according to the hot/cold dissolution process. Therefore, each sample was suspended in water at temperatures above 70 °C with a three-wing stirrer at 500 rpm. These suspensions were then cooled down with ice for 1 h. Afterward, the evaporated water was measured, and additional water was added. These solutions were stored in the refrigerator overnight.

The viscosity shear rate dependence of the solution was investigated with an Anton Paar MCR 501 rheometer. For solutions with a viscosity above 10,000 mPa·s, a cone-plate geometry (CP-50/1°) was chosen, and all other solutions were investigated with a cup and bob setup (CC-27). The viscosity was recorded at 20 °C from 0.1−1000 s^{-1} with 5 measurement points each decade (log scale).

LF-TD-NMR Experiments. A Bruker Minispec mq20 with a ^1H Larmor frequency close to 20 MHz and a magnetic field of 0.47 T, provided with a BVT3000 temperature control unit and gradient unit, has been used for all measurements. The 90° pulse duration is 2.1 μs, the 180° pulse length is 4.1 μs, and the dead time is 14 μs.

200 μL of samples was put in a 6 mm tube, which was sealed with Teflon tape and then inserted into a second NMR tube of 10 mm, sealed with parafilm, to minimize water evaporation. The samples were then put in an ultrasonic bath for 5 min to remove any bubbles that can affect the measurement. Temperature-dependent scans were performed from 300 to 343/353 K in steps of 5 K or less. At each step, the samples were thermalized for about 10 min that was deemed a reasonable time to obtain a constant temperature in the sample.

The determination of the diffusion coefficient of water has been carried out by employing pulsed field gradient (PFG) spin−echo (SE) experiments, following a calibration procedure of gradients with distilled water at 298 K, as detailed elsewhere.[34] The employed parameters are 500 μs as gradient pulse duration and 1 s between the first 90° pulse and the gradient pulse. The diffusion coefficients have been calculated from the slope of the echo signal intensity in the logarithmic scale with respect to the gradients' amplitude to a maximum of 1.45 mT/cm at each temperature. The effect of varying the diffusion time Δ has also been monitored using 7.5 and 2.5 ms as the separation between gradients.

For the measurement of spin−spin relaxation time T_2, the Carr−Purcell−Meiboon−Gill (CPMG)[35] sequence was employed, which has the advantage of reduced experimental time since thousands of echoes are recorded within a single experiment and IS able to suppress the effect of molecular diffusion,[36] whereas for T_1, spin−lattice relaxation time, a saturation recovery (SATREC)[37] sequence was used. To measure the rigid fraction present in the samples after thermogelation, an MSE[38] sequence has been applied. More experimental details regarding the CPMG, SATREC, and MSE sequences can be found in ref 39, whereas fitting details are reported in the Supporting Information.

Analysis of Time-Domain NMR in Gels. Parameters measurable by LF-TD-NMR include self-diffusion coefficient (D), spin−lattice (T_1), and spin−spin (T_2) relaxation times. They are all extremely sensitive to changes in mobility of protons at different time scales[39] and have been extensively employed to study other gels.[40−46]

The self-diffusion coefficient D of a given molecule can be measured by a pulsed field gradient (PFG) spin−echo (SE) technique.[41] The decay of spin−echo signal intensity following the application of

https://doi.org/10.1021/acs.macromol.2c02550
Macromolecules 2023, 56, 4694−4704

magnetic field gradients with increasing intensities is dependent on the scale of self-diffusion.[35] The relationship between the echo amplitude A and gradient intensity is

$$A/A_0 = \exp\left(-\gamma^2\delta^2\left(\Delta - \frac{\delta}{3}\right)DG^2\right) \quad (1)$$

where A_0 is the intensity of the echo without gradients applied, γ is the proton gyromagnetic ratio, δ is the gradient pulse duration, Δ is the diffusion time, and G is the gradient intensity. $(\Delta - \delta/3)$ is a term called effective diffusion time, considering the finite duration of the gradient pulses.[34,46] The mean free path of the probe molecules with respect to the direction of the gradient is given by the Fick's equation $\lambda = \sqrt{2D\Delta}$, where Δ is the NMR experimental diffusion time. The self-diffusion coefficient D of a probe molecule decreases with increasing tortuosity of the molecules' path and can be related to the mesh size of gels, therefore giving information also on the cross-linking degree. In turn, the tortuosity of the gel depends on the size of the molecular probe, so comparing the mobility of different probes can provide a full picture of the gel morphology.[47] One limitation of LF-TD-NMR is that at a low field, the chemical shift resolution is not sufficient to separate different probe molecules, and thus, we will here focus on the diffusion of water.

The relaxation times are instead determined by the mobility over longer time scales. T_2 is basically a monotone function of the autocorrelation time with lower mobility connected with lower T_2, while the dependence of T_1 from molecular dynamics is more complex and also affected by spin diffusion mechanisms, where the presence of relaxation sinks induces the relaxation of the whole system, obtaining in this way faster T_1.[48]

The detection of more than one proton NMR relaxation time can be assigned to the existence of water populations that are separated over the timescale probed, ms for T_2 and up to seconds for T_1, depending on different degrees of interaction with the surrounding environment.[49−51] If the water molecules are instead in a regime of fast exchange, with respect to the time span of the NMR experiment, the relaxation is dynamically balanced between the different states, reducing the relaxation time dispersion and leading to a weighted average time that represents the additive contribution of all of the relaxation sources in the sample. Generally, in hydrogel networks, water is present in two main states: bound solvent molecules, whose motion is restricted and the dipolar interaction with other hydrogen atoms is increased, characterized by a fast relaxation time T_{2b}, and free water molecules, whose relaxation time T_{2f} is longer and closer to the solvent without any solute.[52] For the spin−spin relaxation time, where an exchange between protons of water and solute molecules occurs (which can be considered plausible for cellulose derivatives[53]), we can write

$$\frac{(W_n + W_e)}{T_{2obs}} = \frac{W_b}{T_{2b}} + \frac{W_e}{(T_{2e} + k_e^{-1})} + \frac{W_f}{T_{2f}} \quad (2)$$

where W_n is the total water proton content in the sample, W_b and W_f are the instantaneous interacting (bound) and noninteracting (free) water contents, and T_{2b} and T_{2f} are the intrinsic T_2 relaxation times of the interacting and noninteracting populations. W_e is the fraction of exchangeable MC hydroxyl protons and k_e is the exchange rate constant.[46] Consequently, both T_1 and T_2 give information on the water-binding ability of the molecules and the interaction of water with the surrounding network, providing a vision of the state of MC molecules throughout the process, from solution to gel, and not only in the gel state.

Note that protons with strongly restricted dynamics, e.g., embedded in a rigid/crystalline structure[54] and not exchanging with other hydrogen sources, display relaxation that is too fast for detection through common T_2 sequences. The application of a magic sandwich echo (MSE) block is instead necessary[55−57] to recover the FID (free induction decay) signal lost during the dead time of the instrument. In the theoretical framework of fibrils constituted by 40% semiflexible rod MC chains[58] and 60% water,[23] we would expect a rigid-like signal coming from nonexchanging MC hydrogens and from water molecules embedded in the fibril structure or even strongly bound in an ice-like state over the fibril surface.[59]

RESULTS AND DISCUSSION

The aqueous solutions of methylcellulose (Figure 1) were prepared with the following concentrations: 0.5, 1, 2, 3, 4, and 5% w/w. The viscosities obtained by the flow curves in Figure S1 for the 2% systems are reported in Table 1. While the molecular weight and concentration of MC solutions are varied in this study, the DS and the substitution pattern are kept constant because all MCs are derived from the same starting material by partial degradation.

Table 1. Summary of Sample Viscosity Measured with a Rotational Rheometer on Solutions of 2% w/w Concentration at 2.51 s^{-1}[a]

sample	viscosity [mPa·s]
MC1	5.1
MC2	324
MC3	8213
MC4	50,450

[a]The different viscosities are connected to different molecular weights of the MC molecules. DS = 1.92.

Using rheological and optical methods, the onset of gelation has been determined. In a very dilute system, initial flocculation and chain collapse can be observed visually starting at 327 K. When analyzed as a 2% w/w solution, a steep increase of the storage modulus can be observed at an onset of 331 K. A qualitatively different interaction between the polymer chains and water can be expected in the same range, in line with previous reports.[60]

Diffusion NMR. Diffusion coefficients D determined by PFG-SE for a 2% w/w solution of MC4 are compared with D of pure water in Figure 2. Experiments were conducted between 298 and 338 K at two different diffusion times Δ. The dynamics of water molecules in the MC solution is indistinguishable from pure water at room temperature. Remarkably, even increasing Δ from 2.5 to 7.5 ms does not produce substantial changes in the diffusion coefficient, and the increase of D with temperature is always linear and

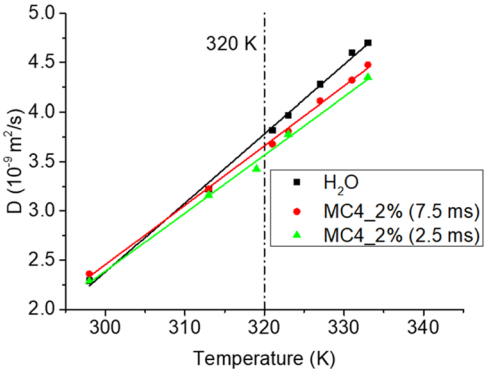

Figure 2. Self-diffusion coefficient of pure water (■, data from literature) and of water solutions of MC4 at 2% w/w at increasing temperature. For MC4 at 2% w/w concentration, two diffusion times Δ are reported (7.5 ms, ●, and 2.5 ms, ▲), and between them, no experimentally significant differences can be appreciated. The dashed line indicates the gel point.

https://doi.org/10.1021/acs.macromol.2c02550
Macromolecules 2023, 56, 4694−4704

unperturbed by gel formation. The temperature dependence of the slope is slightly reduced by the presence of MC4 (Δ = 2.5 ms), resulting in a maximum difference of about 2×10^{-10} m^2/s at 338 K.

This indicates a strongly interconnected water phase around the gel network, which is expected for fibrillar systems.[61] If the fibrils are randomly distributed semiflexible pillars, as previously discussed, they do not strongly hinder molecular diffusion at least for the times probed here. The probability to detect a water molecule reducing its diffusion coefficient because of the interaction with a fibril would be low, in contrast to what happens when single chains or lamellar structures are considered.[62,63]

The mean free path λ of water, estimated using eq 1, is on the order of tens of microns, meaning that the tortuosity of the gel for these MC concentrations is low, and therefore, the gel network is very loose.[64]

MC4 is endowed with the largest molecular weight, and thus, this result can be extended to the other MCs.

We can therefore confirm with this technique that the inhomogeneous arrangement of fibrils[31] subsists at least on the micrometric scale, in line with the nontransparent nature of the resulting gels. Of course, it must be considered that in this work, free diffusing water is dominating because of the low concentrations used. Previous works[65] have in fact highlighted that the hydration level has a strong effect on the measured diffusion coefficient.

NMR Relaxation. The T_2 and T_1 proton relaxation times of the methylcellulose mixtures were measured using CPMG and SATREC sequences, respectively. The CPMG decay curves have been recorded for each sample at a variable temperature from 280 to 353 K, values reasonably above crystallization of water and below its boiling temperature. To better define the transition, the window between 310 and 323 K was sampled at smaller intervals. This choice was justified because microscopic detections of phenomena such as glass transition by TD-NMR customarily precede the macroscopic detection of the same phenomena by several degrees.[66]

Instead, SATREC recovery curves have been recorded only for the highly concentrated solutions on all of the samples, while the sample with the highest molecular weight (MC4) was also measured at concentrations of 1 and 2%.

Most relaxation curves can be accurately fitted by single exponential functions, as expressed in eqs S1 and S2, giving back single ^1H T_1 and ^1H T_2. This confirms that the relaxation process occurs in the fast exchange limit between the water molecule spins even in the gel state. The most concentrated solutions instead present a bimodal transverse decay over 343 K, which will be discussed below in more detail.

The temperature dependence of T_2 is exemplified in Figure 3. At lower temperatures, it starts from a value such as 1300 ms typical of solutions more viscous than pure water and then follows a simple Arrhenius trend, meaning that the water molecular dynamics can be represented by the Blomberg–Purcell–Pound (BPP) relaxation mechanism in the high molecular mobility limit for ^1H T_2, as expected for homogeneous solutions. Approaching the transition temperature, a clear deviation from the increasing exponential trend can be seen, namely, a sharp drop in the ^1H T_2 values between 323 and 333 K (60 °C). This behavior is consistent with the results obtained from the rheology represented in Figure S1. The tipping point represents the TD-NMR transition temperature of the sol–gel process; therefore, the beginning of the transition is slightly shifted (at least 2 °C) to lower temperatures than the one established by more traditional methods.

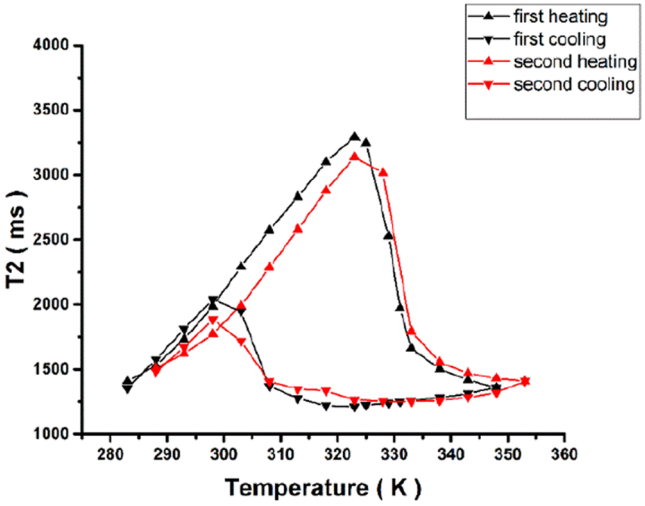

Figure 3. Typical temperature dependence of ^1H T_2 of a solution of MC in water, which can be measured by TD-NMR. The transition from a clear solution to a gel is associated with a drop in the value T_2, here around 325 K. The hysteretic behavior in cooling is also apparent. The repetition of the gelation process highlights that no significant changes occur in the process itself, especially in the gel structure.

The transition is reversible since T_2 returns to the initial value upon cooling to 283 K: a significant hysteresis can be observed during cooling and assigned to the permanence of the metastable gel structure well below the transition temperature determined during heating. Repeating the heating–cooling cycle on the same sample produces results that overlap with the first cycle, with a small systematic decrease of T_2, possibly due to imperfect remixing of small amounts of water expelled from the bulk during gel formation.

The effect of concentration and molecular weight on the transition behavior and on the solution and gel properties was systematically analyzed, as can be seen in Figure 4 and Table 2.

Some general trends can be recognized: at a given concentration, MC solutions characterized by different molecular weights (M_w) present a similar transition temperature. Instead, as visualized in Figure 4, increasing concentration with the same M_w leads to a linearly decreasing transition temperature. Since all samples share the same DS and substituent distribution, the decreasing gel temperature with concentration is easily attributed to the increased probability of interaction and aggregation between chains.

The influence of M_w on water dynamics in solution can be described by the maximum T_2 values attained before the onset of gelation, while the T_2 in the gel state describes its structure and can be related to the strength of the gel itself. Stiffer gels present reduced T_2 values in the sol state because the increased number of interacting sites with water and the higher probability of water bouncing from one interaction site to another are both factors that affect the W_b of eq 2.

The dynamics in the two states are, in principle, independent and can be related by the ε parameter, calculated as $\left(\frac{T_{2,MAX} - T_{2,GEL}}{T_{2,MAX}} \times 100\right) \times \frac{1}{T_{2,GEL}} \times 1000$ (see Table 2). Lower T_2 values in the gel state and the highest percentage variation

https://doi.org/10.1021/acs.macromol.2c02550
Macromolecules 2023, 56, 4694–4704

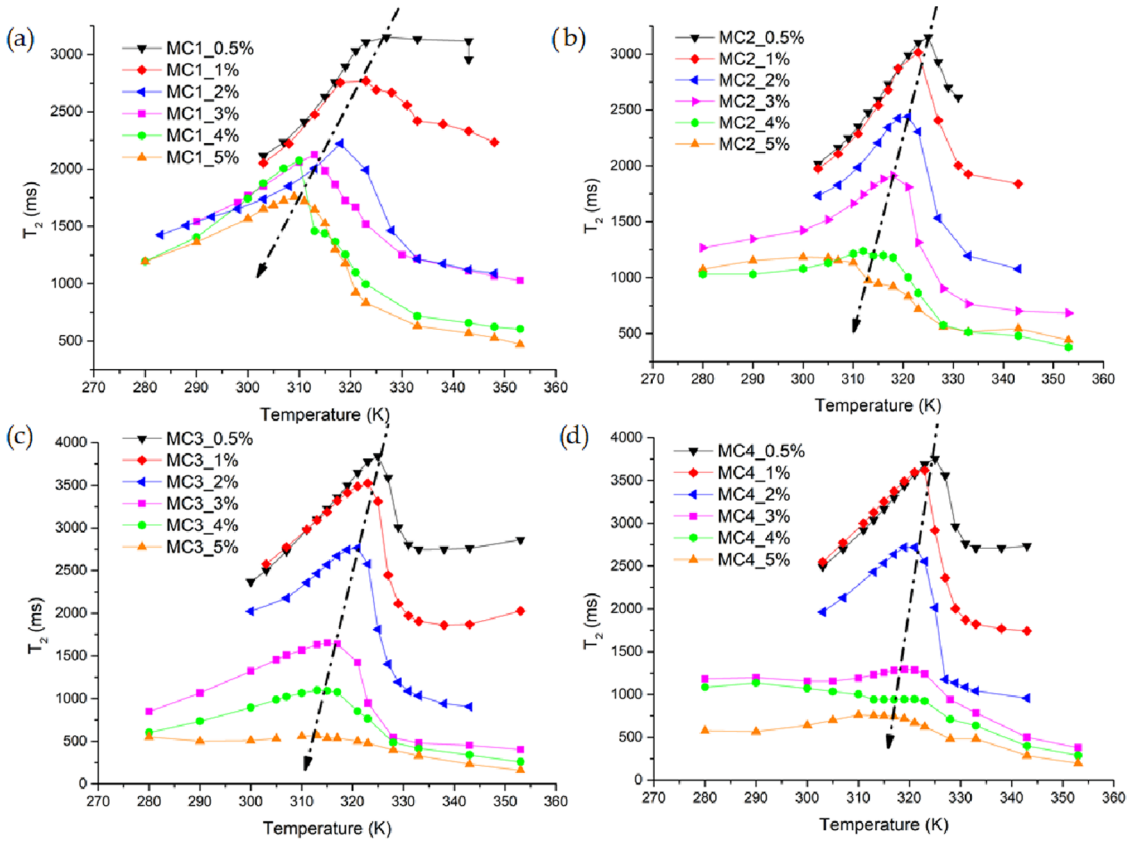

Figure 4. Temperature dependence of ^{1}H T_2, as measured by TD-NMR, of MC1 (a), MC2 (b), MC3 (c), and MC4 (d) at different concentrations. The shifting of the transition temperature for increasing concentration is evidenced by the black arrows.

between the sol and gel state at an increasing concentration indicate the formation of a higher concentration of fibrils that can create a percolated tighter network structure. This parameter can then be interpreted as the efficiency of dehydration and aggregation of MC molecules. It shows a generally increasing value for higher M_w (can be visualized in Figure S3a). Therefore, we could attribute to a higher M_w, a more efficient expulsion of water molecules, deriving from the improved dehydration, and confining effect on solvent molecules, coming from the increased aggregation of chains, meaning the formation of a tighter network. This observation is in accordance with the work of Schmidt et al.,[7] where low M_w MCs create shorter fibrils, which, in principle, entangle poorly, thus limiting water mobility to a minor extent.

The evolution of T_1 as a function of temperature and concentration is displayed in Figure 5a and is likewise consistent with the formation of a low-mobility water population during the sol−gel transition, whose motional correlation time is reduced by the "caging" effect of aggregated MC chains. Pure water, presented for reference in Figure 5a, has a relaxation time that increases with temperature, as predicted for unconstrained motion. At a given temperature, T_1 decreases with MC concentration, and for a given sample, T_1 increases until the gel starts forming. Upon gel formation, T_1 reaches a peak value and then starts decreasing. This is similar to the evolution of T_2 but less dramatic because T_1 is more sensitive to local interactions than T_2, and in this work, the employed MC concentrations are low.[67]

At higher temperatures, when the gel is completely formed, T_1 starts to increase again, at least in the samples with less than 3% MC. One possible cause of such an increase is the formation of highly constrained water population, with τ_c around 10^{-8} s, a value associated with large molecules or solid state. But here the samples where the increase is more pronounced are the ones with less MC content, while in samples with the highest MC concentration, the T_1 actually keeps decreasing up to 353 K. An alternative possibility is the development of anisotropic motion, best discussed by plotting the ratio of T_1 and T_2 (Figure 5b).[41,68] In the case of isotropic dynamics, T_1/T_2 has a value between 1 and 1.6. It is the situation in the region of low temperatures between 300 and 320 K, as can be appreciated in Figure 5b, where, for MC4_1%, it has a value of about 1.2. By further increase of the temperature, an abrupt increase of T_1/T_2 up to 2.8 in the case of MC4_1% can be seen, indicating an increased anisotropy for the water molecular dynamics.

This behavior is similar to what has been observed for water inside poly(*N*-isopropylacrylamide) (PNIPAM) microgels above their lower critical solution temperature (LCST).[42,69] For PNIPAM, the effect on T_2 (and T_1)[70] has been attributed to a dramatic change of confinement state of a fraction of water molecules due to the increased hydrophobic intermolecular interaction between the polymer chains tending to condense into a globular conformation.[71] However, the T_2 values in the gel state of PNIPAM at concentrations like our samples are higher, indicating that the restriction to water motion in those systems is less efficient. Therefore, we can hypothesize a similar constraining effect on water for MC systems, but the association of MC chains to form semicrystalline fibrils[23] can trap a fraction of water molecules in the amorphous phase, constraining their dynamics, thus inducing an even more relevant reduction in $T_{2,b}$ indicated in eq 2. The presence of

https://doi.org/10.1021/acs.macromol.2c02550
Macromolecules 2023, 56, 4694−4704

Table 2. Observed Transition Temperature, T_{rans}, Depending Only on Concentration, Spin−Spin Relaxation Time at the Maximum Point $T_{2,MAX}$, Corresponding to the Transition Temperature, at 333 K, $T_{2,GEL}$, Where the Gel Is Completely Formed, and ε a Parameter Calculated as the Percentage Difference between $T_{2,MAX}$ and $T_{2,GEL}$, Weighted by Its Relaxation Rate[a]

concentration [% w/w]	sample	T_{trans} [K]	$T_{2,MAX}$ [ms]	$T_{2,GEL}$ (@333 K) [K]	ε [%]
0.5	MC1	325	3151	3132	0.2
	MC2		3150	2609	6.6
	MC3		3836	2749	10.3
	MC4		3752	2710	10.2
1	MC1	323	2767	2420	5.2
	MC2		3014	1926	18.7
	MC3		3523	1906	24.1
	MC4		3619	1821	27.3
2	MC1	320	2222	1215	37.3
	MC2		2440	1195	42.7
	MC3		2766	1040	60.0
	MC4		2718	1034	59.9
3	MC1	316	2125	1216	35.2
	MC2		1914	766	78.3
	MC3		1654	480	147.9
	MC4		1294	784	50.3
4	MC1	313	2060	718	90.7
	MC2		1238	515	113.4
	MC3		1097	416	149.2
	MC4		941	635	51.2
5	MC1	310	1758	631	101.6
	MC2		1178	517	108.5
	MC3		570	330	127.6
	MC4		761	482	76.1

[a] M_w is increasing from MC1 to MC4.

bundled rigid structures such as MC crystallites after gelation can provide an additional mechanism of relaxation through their own surface, analogous to solvent relaxation induced by inorganic particles.[72] Water molecules have strong dipolar interaction with surfaces consisting of exposed hydroxyl groups, which is a reasonable assumption even in the case of MC crystallites; therefore, their mobility at the surface becomes greatly restricted. Since we were able to detect only a single exponential in the gel state, we must assume that the trapped and interacting water molecules are anyway able to exchange with free water in the NMR timescale.

Figure 5 also reports how concentration affects T_1 and the T_1/T_2 ratio. T_1 decreases both in the sol and gel phase, indicating a reduction of the tumbling frequency of the molecules. The weak influence of increasing M_w also on T_1 reflects the observations regarding T_2; thus, the network structure of fibrils is similar independently on M_w both at long and short range. The relative behavior of T_1 and T_2 with concentration results in their ratio increasing dramatically in correspondence with the transition, supporting the idea of more hindered water dynamics, restricted by the presence of a higher number of interacting sites due to MC molecules and increased anisotropic behavior after gelation.

Although these observations hold for all of the samples, slightly different behaviors can be observed between the low (<2%) and highly concentrated solutions.

Low Concentration. Below 2% w/w MC, low M_w MC chains have a stronger influence on the T_2 in solution with respect to higher M_w, as can be seen comparing the values of $T_{2\ MAX}$ in Table 2. The lower T_2 of low M_w MC compared to the T_2 of higher M_w MC solutions indicates that low M_w MCs influence the relaxation process of water more strongly. This could happen because of more bound water than for higher M_w, therefore better solvation in solution, which is consistent with lower solubility parameters with increasing molecular weight for polymers.[73] Another possible explanation, which could be even more appealing, can be given referring to the solution behavior of other types of β-glucans[74,75] that form aggregates and clusters at low M_w thanks to higher mobility in solution than high M_w chains. The presence of such clusters could explain the existence of water with lower mobility even in the solution state, whereas the homogeneous distribution of chains in high M_w MC solutions could exert a negligible effect.

T_2 in the gel state is always obtained by a monoexponential function and shows instead a steep decrease at increasing concentration, compatible with the formation of an increasingly homogeneous, structured, and tighter network. Likewise, ε increases almost linearly with concentration and with molecular weight, indicating better aggregation.

High Concentration. At concentrations >2%, the maximum T_2 shows instead a decreasing trend with M_w,

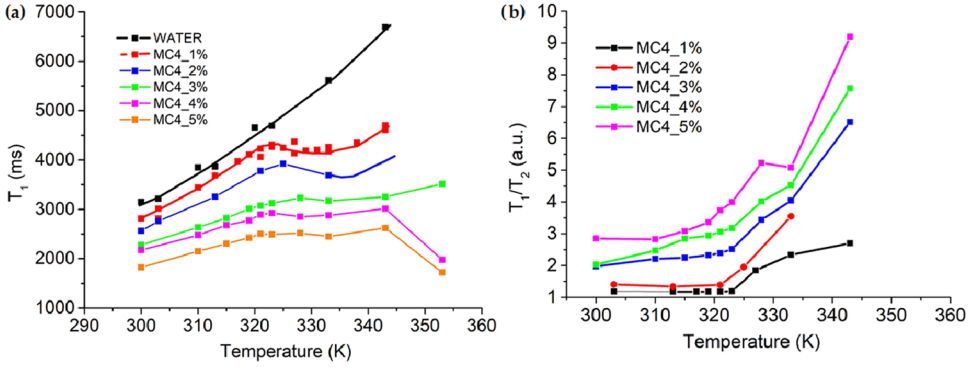

Figure 5. (a) ^{1}H T_1 dependence on temperature for the sample MC4. The transition can be seen as the region spanning from 321 to 333 K, showing a constant or slightly decreasing T_1. The black squares indicate T_1 for deionized water (which are reported for comparison), which continuously increase with increasing temperature. (b) Change in the T_1/T_2 ratio highlights clearly that the solution behaves as an isotropic medium up to the transition temperature, after which an important increase toward a condition of anisotropic motion occurs. The effect is stronger for higher concentration.

https://doi.org/10.1021/acs.macromol.2c02550
Macromolecules 2023, 56, 4694−4704

consistently with increasing viscosity. The deviation from the previous trend can be interpreted with the formation of interactions among the chains also in the solution state because of their high molar number. The possible formation of entanglements among the MC chains with the consequent formation of a network-like structure, as happens in typical polymer solutions above a certain critical concentration, can be responsible for the inversion of trend with respect to the low-concentration region. The significant decrease of T_2 for the high M_w systems, rather than for MC1, which shows little variation with concentration, and the values of the T_1/T_2 ratio >1.6 support this idea. After the transition, T_2 is almost independent of molecular weight and its change with concentration is reduced with respect to the low-concentration regime. It indicates that after the critical concentration, the gel structure remains similar, and the constituted fibrils and their distribution in the space are not much dependent on M_w and concentration, except for a minimal change in the molar number of fibrils in solution, as described by recent literature.[76] By increasing the concentration over 3% w/w, at high temperatures, we could observe the formation of populations with different mobility (Table S1) for all of the samples except MC1. The population with the higher amplitude has a low T_2, which is attributed to the water trapped inside the gel, and the other has a T_2 higher than 1500 ms, which can be attributed to free water expelled by the gel. The extent of the expelled water is determined by the amplitude of the longer T_2 component and by its value: longer the T_2 and higher the amplitude, the more the syneresis. The amplitude of this component and its value increase with increasing concentration and M_w, indicating increasingly effective segregation of MC chains. In other words, the collapsed organization of the gel and the process of water removal can be thought as rather similar for all of the samples under investigation.

Also, T_1 at these concentrations shows a biexponential behavior, indicating the limited spin diffusion between the two water subpopulations. The focus of the present work is the formation of fibrils at low concentrations, but it should be noted that the presence of a multimodal distribution of relaxation times opens the way to further investigation of the higher scales by T_1-T_2 correlation experiments.[77] A separate discussion must be made for MC4. Due to its high M_w, its effect on the aqueous solution is stronger. Thus, ϵ is lower than the other samples at these high concentrations, which can be attributed to the low ΔT_2 between the sol and gel. Moreover, its M_w can be responsible for lower solubility of the chains, preventing a more effective reduction of T_2 with respect to MC3.

MSE Analysis. The observations reported above represent the point of view of the water molecules that constitute at least 95% of all samples. To directly investigate the morphology of the fibrils, we evaluated the possibility of suppressing the water signal via a mobility-based filter but ultimately preferred to avoid the solvent entirely by preparing a sample with 3% w/w MC1 using D_2O that is not detected by ^1H NMR instead of water.

As can be shown in Figure 6, the gel (MSE signal at 343 K) displays a very fast relaxing component at the beginning of the FID, not present in water alone, and negligible in the same sample before gelation. By fitting with eq S3, we could determine that this portion of protons with a strongly hindered solid-like mobility increases with the temperature above

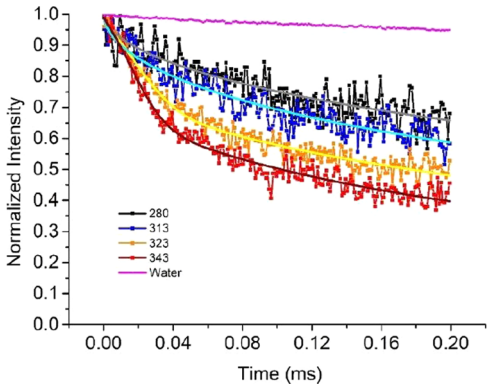

Figure 6. MSE signals that constitute the recovered initial part of the FID of MC1 at increasing temperatures up to complete gelation. The fitting functions are reported as solid lines overlapped with the experimental results. The straight pink line is the signal obtained by pure water as a reference, which does not show any deviation from monoexponential trend.

transition, reaching 23 ± 1% of the signal for the well-formed gel.

To relate proton fraction with phase composition,[78] we have considered that MC with DS 1.92 contains around 14 ^1H per glycosidic unit (molar mass 189 g/mol). We can assume that the exchangeable protons (1.08/unit) will migrate in water and contribute only to the mobile fraction, together with the non-negligible amount (0.1%) of residual protons present in D_2O in the form of HDO. Together, these protons not connected to MC constitute around 12% of the signal intensity. By normalizing the detected rigid fraction against the remaining 88%, we obtain that approx. 26% of MC units are forming a locally rigid phase. These observations are consistent with the hypothesis of a semicrystalline structure of the MC fibrils. The observation, in high-resolution high-field NMR spectra, of Haque et al.[21] of the relevant broadening of the signal of nonexchanging protons of MC indicates a reduced mobility of all of the glycosidic units, and the average values of crystallinity of cellulose (40%) and methylcellulose in the solid state (45−60%) are in accord with our calculation. With respect to the bulk, the structure of MC fibrils is instead constituted mostly by a relatively larger amorphous and water-soaked phase and by a still significant amount of crystalline or more generally strongly constrained portion. Although, at present, we cannot exclude completely the possibility of the presence of water in a state of very strong confinement, which would be plausible if it were included in the crystalline cell, as presented by Lodge et al.[22] in their structure determination through SANS, the detected water participating in the fibril formation could be embedded inside the amorphous fraction of the fibrils, which would be consistent with the possibility for the water molecules to exchange with free water in the NMR time and with the swelling−shrinking process of the fibrils in salty aqueous MC solutions[15] or in cross-linked MC gels as presented by Morozova et al.[79]

In this perspective, the fact that around a quarter of the protons in the fibrils are in a rigid state can explain their semiflexible behavior and the high moduli that can be reached by these gels.

https://doi.org/10.1021/acs.macromol.2c02550
Macromolecules 2023, 56, 4694−4704

CONCLUSIONS

Gelation of MC aqueous solutions has been studied by TD-NMR mainly through the determination of water relaxation times and diffusion coefficients at varying temperatures. Even a relatively inexpensive instrument operating at a low field could measure the typical features of the thermogelation process, including the independence of transition from the molecular weight, its dependence on concentration, and the stiffer gel structure at higher concentrations. Results are well consistent with all other techniques employed so far on such materials. In addition, TD-NMR describes the fibrils as composed mainly by a wet amorphous phase reinforced by rigid regions. The amorphous phase is highly accessible, so the water it contains is in fast dynamic exchange with the bulk.

Indeed, up to at least 2% concentration, self-diffusivity of water is approximately the same as for free water at the tens of micrometer scale even at temperatures where the gel is formed. This is in accord with the idea of a gel network formed by well-distant, inhomogeneously arranged fibrillar structures, with a density not able to influence water diffusion.

The gels show an analogous, although weaker, increase of relaxation rate at increasing MC M_w, which was expected from previous observations regarding longer fibrils with higher M_w. However, we have also observed that M_w significantly impacts water dynamics in the solution state. It is probably a consequence of different aggregation conditions between low and high M_w MC. It results in more efficient dehydration and MC aggregation in high M_w MC solutions, causing more pronounced solvent mobility reduction.

The detection of one average relaxation time for each sample indicates that confined water is almost always in fast exchange with free water. The detection of a rigid fraction that is independent of molecular weight is consistent with a semicrystalline structure of MC in the fibrils, with a crystallinity of no more than 25%.[71] The strong reduction in T_2 and increased T_1/T_2 ratio observed during gelation, considering the concentrations of these systems, are compatible with constrained water mobility in the amorphous part. However, the reduction of water mobility is not enough to prevent the exchange with the outer free water in the NMR timescale (on the order of seconds) and also the instantaneous interactions at the surfaces of crystalline regions.

In other words, our observations support the model inferred by Lodge et al.[29] regarding the semicrystalline amorphous nature of the fibrils. We propose that the bundles are characterized by a semicrystalline rigid, possibly constituted by self-separating fully substituted anhydroglucose unit and of disordered regions lying at the interfaces between crystals, whereas the mobile amorphous part between the bundles represents approximately the majority. Water molecules can diffuse through these amorphous/mobile regions, although they interact strongly, acquiring an important anisotropic motion. This strong interaction can be responsible for the relevant swelling of fibrils that are detected in SANS.[22]

LF-TD-NMR could, therefore, help resolve the possible water compartmentalization that could arise for higher concentrations, and it could also provide more information on the gel network structure performing diffusion experiments with bigger probe molecules and wider MC fraction range. The diffusion behavior could be correlated in fact to the actual gel mesh size or to the flexibility of the fibrils.

In addition, it is fast and inexpensive and requires limited preparation and low amounts of sample, therefore becoming particularly interesting for the analysis of tailored MC samples synthesized with controlled methylation patterns.[80]

ASSOCIATED CONTENT

Supporting Information

The Supporting Information is available free of charge at https://pubs.acs.org/doi/10.1021/acs.macromol.2c02550.

Flow curves of MC solutions; fitting procedure of TD-NMR data; detailed representation of the gelation curves for all of the samples at different concentrations and molecular weights; calculation procedure for the expected rigid fraction of MC fibrils; MSE curves; and R_2 of the gel phase as a function of viscosity (PDF)

AUTHOR INFORMATION

Corresponding Author

Michele Mauri − *Dipartimento di Scienza dei Materiali, Università di Milano-Bicocca, 20125 Milano, Italy;* orcid.org/0000-0002-7777-9820; Email: michele.mauri@unimib.it

Authors

Denise Besghini − *Dipartimento di Scienza dei Materiali, Università di Milano-Bicocca, 20125 Milano, Italy; Trelleborg Printing Solutions Italy S.p.A., 26855 Lodi Vecchio, Lodi, Italy*

Payam Hashemi − *Institute of Food Chemistry, Technische Universität Braunschweig, 38106 Braunschweig, Germany*

Matthias Knarr − *Research & Development, Pharma Solutions, International Flavors & Fragrances (IFF), 29699 Walsrode, Germany*

Roland Adden − *Research & Development, Pharma Solutions, International Flavors & Fragrances (IFF), 29699 Walsrode, Germany*

Petra Mischnick − *Institute of Food Chemistry, Technische Universität Braunschweig, 38106 Braunschweig, Germany*

Roberto Simonutti − *Dipartimento di Scienza dei Materiali, Università di Milano-Bicocca, 20125 Milano, Italy;* orcid.org/0000-0001-8093-517X

Complete contact information is available at: https://pubs.acs.org/10.1021/acs.macromol.2c02550

Author Contributions

M.M., P.M., and R.S. designed the work. D.B. performed and analyzed most of the LF-TD-NMR supported by M.M. P.H. prepared the gels under the guidance of P.M. Methylcellulose synthesis and rheological characterization were performed by M.K. and R.A. The manuscript was written through contributions of all authors.

Notes

The authors declare no competing financial interest.

ACKNOWLEDGMENTS

D.B. thanks Trelleborg Printing Solutions SpA for funding her PhD scholarship. M.M. gratefully acknowledges the support from the Italian Ministry of University and Research (MIUR) through the Dipartimenti di Eccellenza—2019 grant. The authors thank Dr. Massimo Tawfilas and Debora Besghini for their assistance in the realization of the graphical abstract of

the manuscript and Edgar Frexes for the preliminary measurements that opened the path of the whole work.

REFERENCES

(1) Morozova, S.; Schmidt, P. W.; Metaxas, A.; Bates, F. S.; Lodge, T. P.; Dutcher, C. S. Extensional flow behavior of methylcellulose solutions containing fibrils. *ACS Macro Lett.* **2018**, *7*, 347−352.
(2) Jain, S.; Sandhu, P. S.; Malvi, R.; Gupta, B. Cellulose derivatives as thermoresponsive polymer: An overview. *J. Appl. Pharm. Sci.* **2013**, *3*, 139−144.
(3) Nasatto, P.; Pignon, F.; Silveira, J.; Duarte, M.; Noseda, M.; Rinaudo, M. Methylcellulose, a cellulose derivative with original physical properties and extended applications. *Polymers* **2015**, *7*, 777−803.
(4) McAllister, J. W.; Schmidt, P. W.; Dorfman, K. D.; Lodge, T. P.; Bates, F. S. Thermodynamics of aqueous methylcellulose solutions. *Macromolecules* **2015**, *48*, 7205−7215.
(5) Morozova, S. Methylcellulose fibrils: A mini review. *Polym. Int.* **2020**, *69*, 125−130.
(6) Sarkar, N. Thermal gelation properties of methyl and hydroxypropyl methylcellulose. *J. Appl. Polym. Sci.* **1979**, *24*, 1073−1087.
(7) Schmidt, P. W.; Morozova, S.; Owens, P. M.; Adden, R.; Li, Y.; Bates, F. S.; Lodge, T. P. Molecular weight dependence of methylcellulose fibrillar networks. *Macromolecules* **2018**, *51*, 7767−7775.
(8) Funami, T.; Kataoka, Y.; Hiroe, M.; Asai, I.; Takahashi, R.; Nishinari, K. Thermal aggregation of methylcellulose with different molecular weights. *Food Hydrocolloids* **2007**, *21*, 46−58.
(9) Li, L. Thermal gelation of methylcellulose in water: Scaling and thermoreversibility. *Macromolecules* **2002**, *35*, 5990−5998.
(10) Nasatto, P. L.; Pignon, F.; Silveira, J. L. M.; Duarte, M. E. R.; Noseda, M. D.; Rinaudo, M. Influence of molar mass and concentration on the thermogelation of methylcelluloses. *Int. J. Polym. Anal. Charact.* **2015**, *20*, 110−118.
(11) Viridén, A.; Wittgren, B.; Andersson, T.; Abrahmsén-Alami, S.; Larsson, A. Influence of substitution pattern on solution behavior of hydroxypropyl methylcellulose. *Biomacromolecules* **2009**, *10*, 522−529.
(12) Huebner, B.; Knarr, M.; Adden, R.; Sammler Robert, L.; Adden, A. Methods and Compositions for Inducing Satiety. WO Patent WO2013/059065A1, 2013.
(13) Hirrien, M.; Chevillard, C.; Desbrières, J.; Axelos, M. A. V.; Rinaudo, M. Thermogelation of methylcelluloses: New evidence for understanding the gelation mechanism. *Polymer* **1998**, *39*, 6251−6259.
(14) Xu, Y.; Wang, C.; Tam, K. C.; Li, L. Salt-assisted and salt-suppressed sol−gel transitions of methylcellulose in water. *Langmuir* **2004**, *20*, 646−652.
(15) Liberman, L.; Schmidt, P. W.; Coughlin, M. L.; Ya'akobi, A. M.; Davidovich, I.; Edmund, J.; Ertem, S. P.; Morozova, S.; Talmon, Y.; Bates, F. S.; Lodge, T. P. Salt-dependent structure in methylcellulose fibrillar gels. *Macromolecules* **2021**, *54*, 2090−2100.
(16) Li, L.; Thangamathesvaran, P. M.; Yue, C. Y.; Tam, K. C.; Hu, X.; Lam, Y. C. Gel network structure of methylcellulose in water. *Langmuir* **2001**, *17*, 8062−8068.
(17) Miura, Y. Solvent isotope effect on gelation process of methylcellulose studied by nmr and dsc. *Polym. Bull.* **2018**, *75*, 4245−4255.
(18) Heymann, E. Studies on sol-gel transformations. I. The inverse sol-gel transformation of methylcellulose in water. *Trans. Faraday Soc.* **1935**, *31*, 846−864.
(19) Kato, T.; Yokoyama, M.; Takahashi, A. Melting temperatures of thermally reversible gels iv. Methyl cellulose-water gels. *Colloid Polym. Sci.* **1978**, *256*, 15−21.
(20) Kobayashi, K.; Huang, C.-i.; Lodge, T. P. Thermoreversible gelation of aqueous methylcellulose solutions. *Macromolecules* **1999**, *32*, 7070−7077.
(21) Haque, A.; Morris, E. R. Thermogelation of methylcellulose. Part i: Molecular structures and processes. *Carbohydr. Polym.* **1993**, *22*, 161−173.
(22) Lott, J. R.; McAllister, J. W.; Arvidson, S. A.; Bates, F. S.; Lodge, T. P. Fibrillar structure of methylcellulose hydrogels. *Biomacromolecules* **2013**, *14*, 2484−2488.
(23) Lott, J. R.; McAllister, J. W.; Wasbrough, M.; Sammler, R. L.; Bates, F. S.; Lodge, T. P. Fibrillar structure in aqueous methylcellulose solutions and gels. *Macromolecules* **2013**, *46*, 9760−9771.
(24) Bodvik, R.; Dedinaite, A.; Karlson, L.; Bergström, M.; Bäverbäck, P.; Pedersen, J. S.; Edwards, K.; Karlsson, G.; Varga, I.; Claesson, P. M. Aggregation and network formation of aqueous methylcellulose and hydroxypropylmethylcellulose solutions. *Colloids Surf., A* **2010**, *354*, 162−171.
(25) Arvidson, S. A.; Lott, J. R.; McAllister, J. W.; Zhang, J.; Bates, F. S.; Lodge, T. P.; Sammler, R. L.; Li, Y.; Brackhagen, M. Interplay of phase separation and thermoreversible gelation in aqueous methylcellulose solutions. *Macromolecules* **2013**, *46*, 300−309.
(26) Yang, Y.; Wu, W.; Liu, H.; Xu, H.; Zhong, Y.; Zhang, L.; Chen, Z.; Sui, X.; Mao, Z. Aggregation behaviors of thermo-responsive methylcellulose in water: A molecular dynamics simulation study. *J. Mol. Graphics Modell.* **2020**, *97*, No. 107554.
(27) Huang, W.; Dalal, I. S.; Larson, R. G. Analysis of solvation and gelation behavior of methylcellulose using atomistic molecular dynamics simulations. *J. Phys. Chem. B* **2014**, *118*, 13992−14008.
(28) Ginzburg, V. V.; Sammler, R. L.; Huang, W.; Larson, R. G. Anisotropic self-assembly and gelation in aqueous methylcellulose—theory and modeling. *J. Polym. Sci., Part B: Polym. Phys.* **2016**, *54*, 1624−1636.
(29) Schmidt, P. W.; Morozova, S.; Ertem, S. P.; Coughlin, M. L.; Davidovich, I.; Talmon, Y.; Reineke, T. M.; Bates, F. S.; Lodge, T. P. Internal structure of methylcellulose fibrils. *Macromolecules* **2020**, *53*, 398−405.
(30) McAllister, J. W.; Lott, J. R.; Schmidt, P. W.; Sammler, R. L.; Bates, F. S.; Lodge, T. P. Linear and nonlinear rheological behavior of fibrillar methylcellulose hydrogels. *ACS Macro Lett.* **2015**, *4*, 538−542.
(31) Chatterjee, T.; Nakatani, A. I.; Adden, R.; Brackhagen, M.; Redwine, D.; Shen, H.; Li, Y.; Wilson, T.; Sammler, R. L. Structure and properties of aqueous methylcellulose gels by small-angle neutron scattering. *Biomacromolecules* **2012**, *13*, 3355−3369.
(32) Joshi, S. C.; Lam, Y. C.; Bin, C. Modelling leading to water entrapment point in thermally driven hydrogelation of methyl cellulose *e-Polymers* 2008; Vol. *8*, 101.
(33) Villetti, M. A.; Soldi, V.; Rochas, C.; Borsali, R. Phase-separation kinetics and mechanism in a methylcellulose/salt aqueous solution studied by time-resolved small-angle light scattering (sals). *Macromol. Chem. Phys.* **2011**, *212*, 1063−1071.
(34) Ray, S. S.; Rajamohanan, P. R.; Badiger, M. V.; Devotta, I.; Ganapathy, S.; Mashelkar, R. A. Self-diffusion of water in thermoreversible gels near volume transition: Model development and pfg nmr investigation**ncl communication no: 6395. *Chem. Eng. Sci.* **1998**, *53*, 869−877.
(35) Carr, H. Y.; Purcell, E. M. Effects of diffusion on free precession in nuclear magnetic resonance experiments. *Phys. Rev.* **1954**, *94*, 630−638.
(36) Abrami, M.; Chiarappa, G.; Farra, R.; Grassi, G.; Marizza, P.; Grassi, M. Use of low-field nmr for the characterization of gels and biological tissues. *ADMET DMPK* **2018**, *6*, No. 34.
(37) Vismara, E.; Bongio, C.; Coletti, A.; Edelman, R.; Serafini, A.; Mauri, M.; Simonutti, R.; Bertini, S.; Urso, E.; Assaraf, Y.; Livney, Y. Albumin and hyaluronic acid-coated superparamagnetic iron oxide nanoparticles loaded with paclitaxel for biomedical applications. *Molecules* **2017**, *22*, No. 1030.
(38) Mauri, M.; Thomann, Y.; Schneider, H.; Saalwächter, K. Spin-diffusion nmr at low field for the study of multiphase solids. *Solid State Nucl. Magn. Reson.* **2008**, *34*, 125−141.
(39) Besghini, D.; Mauri, M.; Simonutti, R. Time domain nmr in polymer science: From the laboratory to the industry. *Appl. Sci.* **2019**, *9*, No. 1801.

https://doi.org/10.1021/acs.macromol.2c02550
Macromolecules 2023, 56, 4694−4704

(40) McConville, P.; Whittaker, M. K.; Pope, J. M. Water and polymer mobility in hydrogel biomaterials quantified by 1 h nmr: A simple model describing both t1 and t2 relaxation. *Macromolecules* **2002**, *35*, 6961−6969.
(41) Barbucci, R.; Leone, G.; Chiumiento, A.; Di Cocco, M. E.; D'Orazio, G.; Gianferri, R.; Delfini, M. Low- and high-resolution nuclear magnetic resonance (nmr) characterisation of hyaluronan-based native and sulfated hydrogels. *Carbohydr. Res.* **2006**, *341*, 1848−1858.
(42) Sierra-Martín, B.; Romero-Cano, M. S.; Cosgrove, T.; Vincent, B.; Fernández-Barbero, A. Solvent relaxation of swelling pnipam microgels by nmr. *Colloids Surf., A* **2005**, *270-271*, 296−300.
(43) McConville, P.; Pope, J. M. 1 h nmr t2 relaxation in contact lens hydrogels as a probe of water mobility. *Polymer* **2001**, *42*, 3559−3568.
(44) Bastrop, M.; Meister, A.; Metz, H.; Drescher, S.; Dobner, B.; Mäder, K.; Blume, A. Water dynamics in bolaamphiphile hydrogels investigated by 1 h nmr relaxometry and diffusometry. *J. Phys. Chem. B* **2011**, *115*, 14−22.
(45) Valentín, J. L.; López, D.; Hernández, R.; Mijangos, C.; Saalwächter, K. Structure of poly(vinyl alcohol) cryo-hydrogels as studied by proton low-field nmr spectroscopy. *Macromolecules* **2009**, *42*, 263−272.
(46) Barbieri, R.; Quaglia, M.; Delfini, M.; Brosio, E. Investigation of water dynamic behaviour in poly(hema) and poly(hema-co-dhpma) hydrogels by proton t2 relaxation time and self-diffusion coefficient n.M.R. Measurements. *Polymer* **1998**, *39*, 1059−1066.
(47) de Kort, D. W.; Schuster, E.; Hoeben, F. J. M.; Barnes, R.; Emondts, M.; Janssen, H. M.; Lorén, N.; Han, S.; Van As, H.; van Duynhoven, J. P. M. Heterogeneity of network structures and water dynamics in κ-carrageenan gels probed by nanoparticle diffusometry. *Langmuir* **2018**, *34*, 11110−11120.
(48) Grunin, L. Y.; Grunin, Y. B.; Nikolskaya, E. A.; Sheveleva, N. N.; Nikolaev, I. A. An nmr relaxation and spin diffusion study of cellulose structure during water adsorption. *Biophysics* **2017**, *62*, 198−206.
(49) Jepsen, S. M.; Pedersen, H. T.; Engelsen, S. B. Application of chemometrics to low-field 1 h nmr relaxation data of intact fish flesh. *J. Sci. Food Agric.* **1999**, *79*, 1793−1802.
(50) Gianferri, R.; Giampaoli, S.; Magini, V.; Sciubba, F.; Romano Spica, V.; Delfini, M. Study of interaction of water with advanced materials for swimming pool sportswear by nmr spectroscopy. *Microchem. J.* **2014**, *112*, 132−136.
(51) Le Botlan, D.; Rugraff, Y.; Martin, C.; Colonna, P. Quantitative determination of bound water in wheat starch by time domain nmr spectroscopy. *Carbohydr. Res.* **1998**, *308*, 29−36.
(52) Van der Beek, G. P.; Stuart, M. A. C.; Cosgrove, T. Polymer adsorption and desorption studies via proton nmr relaxation of the solvent. *Langmuir* **1991**, *7*, 327−334.
(53) Ibbett, R.; Wortmann, F.; Varga, K.; Schuster, K. C. A morphological interpretation of water chemical exchange and mobility in cellulose materials derived from proton nmr t2 relaxation. *Cellulose* **2014**, *21*, 139−152.
(54) Räntzsch, V.; Haas, M.; Özen, M. B.; Ratzsch, K.-F.; Riazi, K.; Kauffmann-Weiss, S.; Palacios, J. K.; Müller, A. J.; Vittorias, I.; Guthausen, G.; Wilhelm, M. Polymer crystallinity and crystallization kinetics via benchtop 1 h nmr relaxometry: Revisited method, data analysis, and experiments on common polymers. *Polymer* **2018**, *145*, 162−173.
(55) Maus, A.; Hertlein, C.; Saalwächter, K. A robust proton nmr method to investigate hard/soft ratios, crystallinity, and component mobility in polymers. *Macromol. Chem. Phys.* **2006**, *207*, 1150−1158.
(56) Meyer, H. W.; Schneider, H.; Saalwächter, K. Proton nmr spin-diffusion studies of ps-pb block copolymers at low field: Two- vs three-phase model and recalibration of spin-diffusion coefficients. *Polym. J.* **2012**, *44*, 748−756.
(57) Schäler, K.; Roos, M.; Micke, P.; Golitsyn, Y.; Seidlitz, A.; Thurn-Albrecht, T.; Schneider, H.; Hempel, G.; Saalwächter, K. Basic principles of static proton low-resolution spin diffusion nmr in nanophase-separated materials with mobility contrast. *Solid State Nucl. Magn. Reson.* **2015**, *72*, 50−63.
(58) Arai, K.; Horikawa, Y.; Shikata, T.; Iwase, H. Reconsideration of the conformation of methyl cellulose and hydroxypropyl methyl cellulose ethers in aqueous solution. *RSC Adv.* **2020**, *10*, 19059−19066.
(59) Boral, S.; Bohidar, H. B. Effect of water structure on gelation of agar in glycerol solutions and phase diagram of agar organogels. *J. Phys. Chem. B* **2012**, *116*, 7113−7121.
(60) Sammler, R.; Mohler, C.; Adden, R.; Brackhagen, M.; Moore, J.; Huebner-Keese, B. Control of Gelation and Syneresis of Aqueous Cellulosic Ether Materials. In *Abstracts of Papers of the American Chemical Society*; AMER CHEMICAL SOC: 1155 16TH ST, NW, WASHINGTON, DC 20036 USA, 2017.
(61) Veres, P.; Kéri, M.; Bányai, I.; Lázár, I.; Fábián, I.; Domingo, C.; Kalmár, J. Mechanism of drug release from silica-gelatin aerogel—relationship between matrix structure and release kinetics. *Colloids Surf., B* **2017**, *152*, 229−237.
(62) Quesada-Pérez, M.; Martín-Molina, A. Solute diffusion in gels: Thirty years of simulations. *Adv. Colloid Interface Sci.* **2021**, *287*, No. 102320.
(63) Johansson, L.; Skantze, U.; Loefroth, J. E. Diffusion and interaction in gels and solutions. 2. Experimental results on the obstruction effect. *Macromolecules* **1991**, *24*, 6019−6023.
(64) Kharbanda, Y.; Urbańczyk, M.; Laitinen, O.; Kling, K.; Pallaspuro, S.; Komulainen, S.; Liimatainen, H.; Telkki, V.-V. Comprehensive nmr analysis of pore structures in superabsorbing cellulose nanofiber aerogels. *J. Phys. Chem. C* **2019**, *123*, 30986−30995.
(65) Lázár, I.; Forgács, A.; Horváth, A.; Király, G.; Nagy, G.; Len, A.; Dudás, Z.; Papp, V.; Balogh, Z.; Moldován, K.; et al. Mechanism of hydration of biocompatible silica-casein aerogels probed by nmr and sans reveal backbone rigidity. *Appl. Surf. Sci.* **2020**, *531*, No. 147232.
(66) Bonetti, S.; Farina, M.; Mauri, M.; Koynov, K.; Butt, H. J.; Kappl, M.; Simonutti, R. Core@shell poly(n-butylacrylate)@poly-styrene nanoparticles: Baroplastic force-responsiveness in presence of strong phase separation. *Macromol. Rapid Commun.* **2016**, *37*, 584−589.
(67) Szuminska, K.; Gutsze, A.; Kowalczyk, A. Relaxation of water protons in highly concentrated aqueous protein systems studied by nmr spectroscopy. *Z. Naturforsch., C* **2001**, *56*, 1075−1081.
(68) Carenza, M.; Cojazzi, G.; Bracci, B.; Lendinara, L.; Vitali, L.; Zincani, M.; Yoshida, M.; Katakai, R.; Takacs, E.; Higa, O. Z.; Martellini, F. The state of water in thermoresponsive poly(acryloyl-l-proline methyl ester) hydrogels observed by dsc and 1 h-nmr relaxometry. *Radiat. Phys. Chem.* **1999**, *55*, 209−218.
(69) Yoshioka, H.; Mori, Y.; Cushman, J. A. A synthetic hydrogel with thermoreversible gelation, iii: An nmr study of the sol−gel transition. *Polym. Adv. Technol.* **1994**, *5*, 122−127.
(70) Ohta, H.; Ando, I.; Fujishige, S.; Kubota, K. Molecular motion and 1 h nmr relaxation of aqueous poly(n-isopropylacrylamide) solution under high pressure. *J. Polym. Sci., Part B: Polym. Phys.* **1991**, *29*, 963−968.
(71) Deshmukh, S. A.; Sankaranarayanan, S. K. R. S.; Suthar, K.; Mancini, D. C. Role of solvation dynamics and local ordering of water in inducing conformational transitions in poly(n-isopropylacrylamide) oligomers through the lcst. *J. Phys. Chem. B* **2012**, *116*, 2651−2663.
(72) Tawfilas, M.; Mauri, M.; De Trizio, L.; Lorenzi, R.; Simonutti, R. Surface characterization of tio2 polymorphic nanocrystals through 1 h-td-nmr. *Langmuir* **2018**, *34*, 9460−9469.
(73) Adamska, K.; Voelkel, A. Hansen solubility parameters for polyethylene glycols by inverse gas chromatography. *J. Chromatogr. A* **2006**, *1132*, 260−267.
(74) Zielke, C.; Lu, Y.; Nilsson, L. Aggregation and microstructure of cereal β-glucan and its association with other biomolecules. *Colloids Surf., A* **2019**, *560*, 402−409.
(75) Wu, J.; Zhao, L.; Li, J.; Jin, S.; Wu, S. Aggregation and gelation of oat β-glucan in aqueous solution probed by nmr relaxometry. *Carbohydr. Polym.* **2017**, *163*, 170−180.

https://doi.org/10.1021/acs.macromol.2c02550
Macromolecules 2023, 56, 4694−4704

(76) Coughlin, M. L.; Liberman, L.; Ertem, S. P.; Edmund, J.; Bates, F. S.; Lodge, T. P. Methyl cellulose solutions and gels: Fibril formation and gelation properties. *Prog. Polym. Sci.* **2021**, *112*, No. 101324.
(77) Jaeger, F.; Shchegolikhina, A.; Van As, H.; Schaumann, G. E. Proton NMR Relaxometry as a Useful Tool to Evaluate Swelling Processes in Peat Soils. *Open Magn. Reson. J.* **2010**, *3*, 27−45.
(78) Mauri, M.; Dibbanti, M. K.; Calzavara, M.; Mauri, L.; Simonutti, R.; Causin, V. Time domain nuclear magnetic resonance: A key complementary technique for the forensic differentiation of foam traces. *Anal. Methods* **2013**, *5*, 4336−4344.
(79) Morozova, S.; Coughlin, M. L.; Early, J. T.; Ertem, S. P.; Reineke, T. M.; Bates, F. S.; Lodge, T. P. Properties of chemically cross-linked methylcellulose gels. *Macromolecules* **2019**, *52*, 7740−7748.
(80) Hashemi, P.; Mischnick, P. 1,4-d-glucan block copolymers: Synthesis and comprehensive structural characterization. *Anal. Bioanal. Chem.* **2020**, *412*, 1597−1610.

https://doi.org/10.1021/acs.macromol.2c02550
Macromolecules 2023, 56, 4694−4704